Analytical Investigation of Free Vibrations in Functionally Graded Material Beams with Different Property Distributions

A. Elhannani[1], R. Brahami[2], A. Elmeiche[3], M. Bouamama[2], A Rabehi[4], M. Benghanem[5,*]

[1]Faculty of Science and Technology, Tissemsilt University, Tissemsilt, Algeria.
[1]Laboratory of Electronics, Computer Science and Applied Mathematics (LEIMA), Faculty of Science and Technology, Tissemsilt University, Tissemsilt, Algeria.
[2]Center of Research in Mechanics (CRM), BP N73B, Ain El Bey, Constantine, Algeria.
[3]Laboratory of solids and structures mechanics, University of Sidi-BelAbbes, Algeria.
[4] Laboratory of Telecommunication and Smart Systems (LTSS), Faculty of Science and Technology, University of Djelfa, Algeria
[5]Physics Department, Faculty of Science, Islamic University of Madinah, Madinah, Saudi Arabia.

ABSTRACT: This study focuses on the analysis of the vibrational behavior of functionally graded material (FGM) beams, characterized by continuously varying mechanical properties along their thickness. Emphasis is placed on understanding the free vibrations of these structures and determining their eigenfrequencies using the Euler-Bernoulli beam model. The study considers several boundary conditions to evaluate the influence of material property variations on the beam's dynamics. Three types of distributions are considered to describe the evolution of material properties: the power-law distribution (P-FGM), the exponential distribution (E-FGM), and the sigmoid distribution (S-FGM). This approach allows for a better understanding of the effect of each gradient type on the vibrational performance of the FGM beams and optimizes their design for various engineering applications. The principle of virtual work is applied to establish the equation of motion, and an eigenvalue problem is solved to determine the solutions. The comparison of numerical results with those found in the literature validates the proposed model, confirming its accuracy for the case of an E-FGM beam. Numerous studies are conducted to analyze the impact of the material property distributions on eigenfrequencies, considering various vibration modes and different boundary conditions.

KEYWORDS: Vibratory Analysis, Beams, Functionally Graded Materials (Fgm), Eigenfrequencies, Property Gradients.

[Received Mar. 23, 2025; Revised April 30, 2025; Accepted May 14, 2025] Print ISSN: 0189-9546 | Online ISSN: 2437-2110

I. INTRODUCTION

Vibration analysis of structures is important in engineering for a variety of reasons. It allows for the exact identification of eigenfrequencies vibration frequencies, hence avoiding the hazards of damaging resonance. Furthermore, it assesses the corresponding vibration modes, providing a thorough view of motions and dynamic behaviors. This study is critical for determining the structure's capacity to sustain dynamic loads such as severe winds, earthquakes, and machine-induced vibration. It also helps to optimize the design by reducing undesired vibrations and increasing overall robustness (Elmeiche *et al.*, 2022).

According to current study, functional gradient structures (FGM) are known for their extraordinary capacity to increase mechanical and thermal characteristics while varying their composition and microstructure. Numerous investigations have been conducted on the mechanical and thermal properties of these materials (Ma *et al.*, 2023; Das *et al.*, 2024; Liu *et al.*, 2024). However, research on the dynamic investigations of structures in FGM remains restricted, with a concentration on theoretical elements. The free vibrations of the FG-beams in various boundary condition configurations are investigated using Euler-Bernoulli (EBT), Timoshenko, and third-order theories, which account for changes in material characteristics as beam thickness rises (Mishra *et al.*, 2023; Karabulut *et al.*, 2023). Researchers investigated the static and dynamic behavior of FG-beams in a variety of conditions. These studies investigate how graded mechanical and thermal parameters affect beam response under various environmental circumstances (Esen, 2019; Quang *et al.,* 2021; Priyanka *et al.,* 2022; Bagheri *et al.,* 2023; Gayen, 2024).

The beam is regarded as one of the most common structural components, playing an important role in the design of numerous structures and machine parts. As a result, studying their static and dynamic behavior has become increasingly important (Tüfekci *et al.*, 2024). Numerous research has looked at the free and forced vibrations of beams made of functional gradient materials (FGM), which are employed as structural components in a range of architectural applications. Chikh (2019) investigated the static behavior of the P-FGM beam enhanced by Navier's solution, presenting and comparing the numerical results of the novel shear models to those in the literature to assess the influence of geometry and mixing law. Hadji *et al.* (2016) proposed a unique first-order shear

*Corresponding author: *mbenghanem@iu.edu.sa*
doi: http://dx.doi.org/10.63746/njtd.v22i3.3530

deformation theory for functionally graded beams. By eliminating the stretching-bending coupling effect with a neutral surface, this theory lowers the equations and boundary conditions to those of isotropic plates. By comparing this theory to existing solutions, its correctness is proved. Su *et al.* (2024) used Euler-Bernoulli beam theory and the transfer matrix method (TMM) to investigate the dynamic behavior of beams in FGM under various boundary conditions. They validated their findings with ABAQUS simulations after evaluating the forced and free vibrations of the beams at three and five levels. Their study illustrates the precision and usefulness of TMM by analyzing frequencies and dynamic responses parametrically (Elhannani *et al.*, 2019). Their study focuses on the vibrational analysis of a rotating conical shaft in materials with property gradients (FGM). Applying the Timoshenko beam theory (FSDBT) while accounting for rotational inertia and gyroscopic effects. According to the exponential law (E-FGM), material characteristics vary constantly as the thickness of a hollow shaft increases. Their work aims to determine how the shaft's taper and the distribution of the two extreme materials effect the dynamic behavior of conical rotors in FGM.

This work makes the following main contributions:

- Developed an analytical model using Euler-Bernoulli beam theory to investigate the free vibration behavior of Functionally Graded Material (FGM) beams. This model is adaptable to a variety of boundary conditions, making it useful for actual engineering applications;
- Comparing three types of FGM beams: power-law (P-FGM), exponential (E-FGM), and sigmoid (S-FGM) distributions. This comparison analysis provides useful information about how different material property distributions affect the vibrational properties of FGM beams;
- Our suggested model was validated by comparing findings to existing literature, exhibiting accuracy and dependability. This validation assures that our findings are scientifically sound and may serve as a reference for future research;
- Investigating how the material gradient index "p" affects the eigenfrequencies of FGM beams. This research gives a better knowledge of how material composition influences vibrational behavior, which is important for improving FGM designs;
- FGM beams are widely employed in aerospace, automotive, and civil engineering because to their exceptional mechanical qualities.

The originality of our current effort lies in the following outcomes:

- This study examines three types of female genital mutilation (P-FGM, E-FGM, and S-FGM), unlike prior research that only examined one. This multifaceted approach leads to a more complete knowledge of FGM behavior;
- This study focuses on the characteristics of free vibrations of FG-beams considered as a key element in the analysis of structural dynamics. The application of the principle of virtual work combined with the resolution of an eigenvalue problem to determine the Eigen frequencies, constitutes an innovative approach in this field;
- By analyzing the influence of the volume fraction parameter "p", this work revealed how the combination of ceramic and metal phases affects the eigenfrequencies. This insight is particularly novel for S-FGM beams, where the effect of "p" was found to be less pronounced compared to P-FGM beams;
- This work includes a comparison of FGM beams with isotropic beams, highlighting the unique advantages of the FGMs in terms of vibrational performance. This comparison is novel and underscores the potential of FGMs in advanced engineering applications.
- Results show that E-FGM beams exhibit lower eigen frequencies compared to S-FGM and P-FGM beams. This finding is novel and contributes to the understanding of how exponential material distributions influence vibrational behavior;

The rest of the paper is arranged as follows: Section 2 discusses the material features of P-FGM, S-FGM, and E-FGM. 1. Section 3 covers mathematical formulations. Section 4 includes the numerical results and comments. Finally, the conclusion is summarized in Section 5.

II. MATERIAL CHARACTERISTICS FOR POWER-LAW GRADIENT (P-FGM), SIGMOID GRADIENT (S-FGM) AND EXPONENTIAL GRADIENT (E-FGM) DISTRIBUTIONS.

The coordinates “x” and “y” define the plane of the beam, while the axis “z” oriented along the medial surface corresponds to the thickness direction (Figure. 1). The material characteristics, such as the modulus of elasticity “E”, the density “ρ” and the Poisson ratio “ν”, vary continuously as a function of the thickness “h” according to the volume distribution function adopted.

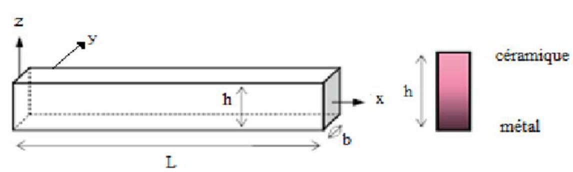

Figure 1. Coordinates and dimensions of the FGM beam

The volume fraction P-FGM is assumed to obey a power function law (Chi and Chung, 2006).

$$g(z)=\left(\frac{z+\frac{h}{2}}{h}\right)^{P} \tag{1}$$

Where

$g\ (z)$: Volume fraction.

p: Volume fraction index.

h: Beam thickness.

z: The coordinate through the thickness.

Once the local volume fraction g(z) is established, the material characteristics of a P-FGM beam may be derived using the law of mixtures:

$$E(z)=g(z).E_1+\left[1-g(z)\right]E_2 \tag{2}$$

Where E_2 and E_1 denote the material properties (elastic modulus, density and Poisson's ratio) of the bottom (z = -h/2) and top (z = +h/2) surfaces of the functionally graded beam (FGM).

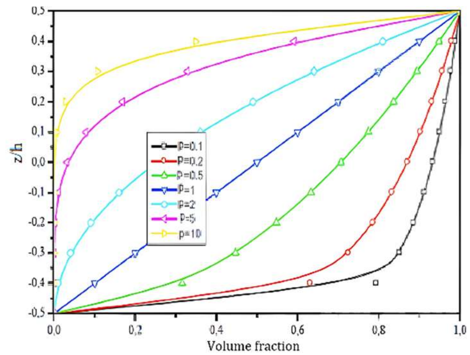

Figure 2. The variation of the material properties in a P–FGM beam.

Chi and Chung (2006) calculated the volume fraction of the FGM beam using two power functions, ensuring a homogeneous stress distribution on all surfaces. The definitions of these two functions are as follows:

$$g_1(z)=1-\frac{1}{2}\left(\frac{\frac{h}{2}-z}{\frac{h}{2}}\right)^P \quad \text{for} \quad 0\le z\le h/2 \tag{3}$$

$$g_2(z)=\frac{1}{2}\left(\frac{\frac{h}{2}+z}{\frac{h}{2}}\right)^P \quad \text{for} \quad -h/2\le z\le 0 \tag{4}$$

Using the law of mixtures, the E property of the S-FGM beam may be determined as:

$$E(z)=g_1(z).E_1+\left[1-g_1(z)\right]E_2 \quad \text{for} \quad 0\le z\le h/2 \tag{5}$$

$$E(z)=g_2(z).E_1+\left[1-g_2(z)\right]E_2 \quad \text{for} \quad -h/2\le z\le 0 \tag{6}$$

Figure. 3 illustrates the variation of material properties along the thickness of the S-FGM beam for various values of "p".

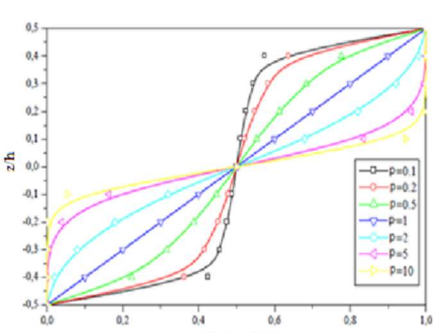

Figure 3. Variation of material characteristics in an S-FGM beam.

Many studies utilize the exponential function to characterize the physical features of FGM materials. The exponential function is defined by (Delale and Erdogan, 1983).

$$E(z)=A.e^{\beta(z+h/2)} \tag{7}$$

with $\quad A=E_2 \quad$ and $\quad \beta=\frac{1}{h}\ln\left(\frac{E_1}{E_2}\right)$

Figure 4 shows the material properties, including the elastic modulus, as a function of the thickness of the E-FGM beam.

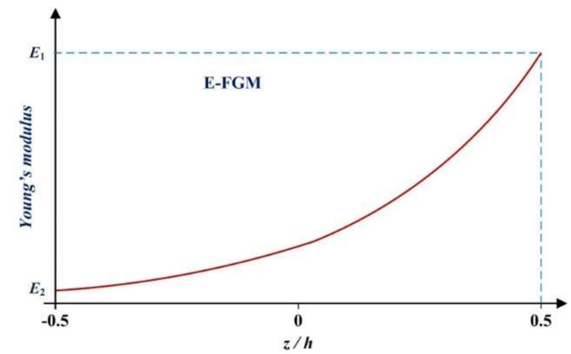

Figure 4. Variations in the Young's modulus of the E-FGM beam.

The modification of the Young's modulus is accomplished utilizing a single function that dominates the material distribution in the E-FGM beam.

III. MATHEMATICAL FORMULATIONS

The equilibrium equations can be formulated using the principle of virtual work. In the static regime, equilibrium is defined by the equality between internal work (δWint) and external work (δWext) induced by the displacement field of the point under study. Thus, the sum of the virtual efforts of the internal and external actions exerted on the system is zero (Mechab, 2011).

$$\delta W_{ext}(\delta U)+\delta W_{int}(\delta U)=0,\ \forall(\delta U) \tag{8}$$

$$\delta W_{int}=-\iint\int_0^L \sigma_{xx}\delta\varepsilon_{xx}dV \tag{9}$$

$$\delta W_{int}=-\iint\int_0^L \sigma_{xx}\left(\delta u_{0,x}-z\delta w_{,xx}\right)dx\,dy\,dz \tag{10}$$

$$\delta W_{int}=-\iint\int_0^L \sigma_{xx}\delta u_{0,x}dx\,dy\,dz+\iint\int_0^L \sigma_{xx}z\delta w_{,xx}dx\,dy\,dz \tag{11}$$

$$\delta W_{int}=-\int_0^L N(x)\delta u_{0,x}dx+\int_0^L M(x)\delta w_{,xx}dx \tag{12}$$

Such as:

N(x): The normal effort to the point x;

$$N(x)=\iint\sigma_{xx}dy\,dz \tag{13}$$

M(x): The bending moment at the point x;

$$M(x)=\iint_{xx}\sigma_{xx}z\,dy\,dz \tag{14}$$

$$N(x)=b\int_{-\frac{h}{2}}^{+\frac{h}{2}}Q_{11}\frac{\partial u_0}{\partial x}dz-b\int_{-\frac{h}{2}}^{+\frac{h}{2}}Q_{11}\,z\frac{\partial^2 w}{\partial x^2}dz \tag{15}$$

Where:

$$Q_{11}=\frac{E(z)}{1-\nu^2}$$

$$N(x)=bA_{11}\frac{\partial u_0}{\partial x}-bB_{11}\frac{\partial^2 w}{\partial x^2} \tag{16}$$

Such as:

$$(A_{11},B_{11},D_{11})=\int_{-\frac{h}{2}}^{+\frac{h}{2}}Q_{11}\left(1,z,z^2\right)dz \tag{17}$$

$$M(x)=b\frac{\partial u_0}{\partial x}\int_{-\frac{h}{2}}^{+\frac{h}{2}}Q_{11}\,zdz-b\frac{\partial^2 w}{\partial x^2}\int_{-\frac{h}{2}}^{+\frac{h}{2}}Q_{11}\,z^2dz \tag{18}$$

$$M(x)=bB_{11}\frac{\partial u_0}{\partial x}-bD_{11}\frac{\partial^2 w}{\partial x^2} \tag{19}$$

The two expressions (16) and (19) can be written in matrix form:

$$\begin{Bmatrix}N\\M\end{Bmatrix}=b\begin{bmatrix}A_{11} & B_{11}\\ B_{11} & D_{11}\end{bmatrix}\begin{Bmatrix}\varepsilon_0\\k_x\end{Bmatrix} \tag{20}$$

with:

- The normal deformation is given by: $\varepsilon_0=\frac{\partial u_0}{\partial x}$
- The bending curvature is given by: $K_x=\frac{\partial^2 w}{\partial x^2}$

The work of external efforts is written:

$$\delta W_{ext}(\delta U)=\int_V f^V\,\delta U dV+\int_s f^S\,\delta U\,ds \tag{21}$$

$$W_{ext}=b\iint_0^L\rho(z)\ddot{w}\,\delta w dxdz$$

$$W_{ext}=b\int_0^L I_1\ddot{w}\,\delta w dx \tag{22}$$

Such as:

I_1: Function of the volume fraction, $I_1=\int_{-\frac{h}{2}}^{+\frac{h}{2}}\rho(z)dz$

Substituting equations (12) and (22) in (8), we obtain:

$$b\int_0^L I_1\ddot{w}\,\delta w dx-\int_0^L N(x)\,\delta u_{0,x}dx+\int_0^L M(x)\,\delta w_{,xx}dx=0 \tag{23}$$

$$\begin{cases}A_{11}\dfrac{\partial^2 u_0(x,t)}{\partial x^2}-B_{11}\dfrac{\partial^3 w(x,t)}{\partial x^3}=0 & (24a)\\[2ex] B_{11}\dfrac{\partial^3 u_0(x,t)}{\partial x^3}-D_{11}\dfrac{\partial^4 w(x,t)}{\partial x^4}+I_1\,w(\ddot{x},t)=0 & (24b)\end{cases}$$

By replacing equation (24a) in (24b), the following general equation is obtained:

$$\xi_j\frac{\partial^4 w(x,t)}{\partial x^4}+w(\ddot{x},t)=0 \tag{25}$$

Such as:

$$\xi_j=\frac{1}{I_1}\left(\frac{B_{11}{}^2}{A_{11}}-D_{11}\right);\quad \text{j= S-FGM; P-FGM; E-FGM}$$

In the case of harmonic vibrations, the displacement can be expressed in mathematical form as shown below:

$$(x,t)=w(x).e^{i\omega t} \tag{26}$$

ω: is the eigenfrequency of the FG-beam.

Replacing equation (26) in equation (25), we obtain the following ordinary differential equation:

$$\frac{d^4 w(x)}{dx^4}-\beta^4\,w(x)=0 \tag{27}$$

β_n is the wave number;

$$\beta_n=\sqrt[4]{\frac{\omega_n{}^2}{\xi_j}}\qquad \text{j= S-FGM; P-FGM; E-FGM}$$

this work, we analyze beams with four distinct support configurations: a beam clamped at both ends (C-C), a beam hinged at one end and clamped at the other (C-S), a beam hinged at both ends (S-S) and a beam clamped at one end and free at the other (C-F). The boundary condition associated with these configurations are defined as follows:

1. Clamped-Clamped beam (C-C):

$$\begin{cases}w_n(\tau)=w_n^{'}(\tau)=0 & \tau=0\\ w_n(\tau)=w_n^{'}(\tau)=0 & \tau=1\end{cases} \tag{28}$$

2. C - S: clamped – supported beam:

$$\begin{cases}w_n(\tau)=w_n^{'}(\tau)=0 & \tau=0\\ w_n(\tau)=w_n^{''}(\tau)=0 & \tau=1\end{cases} \tag{29}$$

3. S - S: supported – supported beam:

$$\begin{cases}w_n(\tau)=w_n^{''}(\tau)=0 & \tau=0\\ w_n(\tau)=w_n^{''}(\tau)=0 & \tau=1\end{cases} \tag{30}$$

4. Clamped – free beam (C-F):

$$\begin{cases}w_n(\tau)=w_n^{'}(\tau)=0 & \tau=0\\ w_n^{''}(\tau)=w_n^{'''}(\tau)=0 & \tau=1\end{cases} \tag{31}$$

For each mode, the eigenfrequencies is given by:

$$\omega_n=(\beta_n/L)^2\,.\sqrt{\xi_j}\quad \text{j=S-FGM;P-FGM; E-FGM} \tag{32}$$

IV. NUMERICAL RESULTS AND DISCUSSION

In the current investigation, the functional gradient beam (FG-beam) is assumed to be constituted up of 100% metal on the upper surface (+h/2) and 100% ceramic Al2O3 on the lower surface (-h/2). The mechanical properties of these two materials are summarized in Table 1.

Table1. Mechanical characteristics between the two materials

Material	Property		
	E(GPa)	***Density ρ (kg/m³)***	***Poisson's ratio v***
Aluminium *(Al)*	70	2780	0.33
Alumina *(Al_2O_3)*	380	3800	0.33

The dimensions of the beam are given as follows:
h = 10 cm; The ratio of length to thickness L/h =10;
The parameters used in this study were selected to match practical engineering applications, particularly in aerospace and mechanical structures where functionally graded materials (FGMs) are increasingly used. Beam dimensions and material properties, such as Young's modulus, density, and Poisson's ratio, were adopted from widely used FGM systems (e.g., aluminum-alumina or steel-zirconia composites) and validated by previous experimental and numerical studies (Dong, W.; Liu, Y. and Xiang, Z., 2012). These choices ensure that the model represents both the mechanical behavior and practical constraints encountered in real-life applications.

The numerical results are expressed in normalized frequencies. The non-dimensional eigenfrequency parameter is formulated as follows:

$$\bar{\omega}_n = \omega_n / \sqrt{\xi_0}$$

Knowing that:
The value of ξ0 will be expressed for the case of an isotropic and homogeneous beam whose stiffness ratio $E_1/E_2=1$ (E_2 and E_1 are respectively the rigidities of the two lower and upper interfaces). The results presented here provide analytical solutions that make it possible to describe the vibratory behavior of the FGM beams for different boundary conditions that were obtained after solving equation (25).
Table 2 shows the first three normalized frequencies ($\overline{\omega_n}$) of an E-FGM beam with a combination of aluminum (Al) and alumina (Al_2O_3), according to the exponential distribution function, for various boundary conditions and stiffness ratios.

$$E_1/E_2 = 0.2,\ 1,\ 5.$$

Table 2. First dimensionless frequencies ($\overline{\omega_n}$) of a uniform beam in E-FGM material.

$\frac{E_1}{E_2}$	$\overline{\omega_n}$	C-C Present	C-C (Dong, W. and al. ,2012)	C-S Present	C-S (Dong, W. and al. ,2012)	S-S Present	S-S (Dong, W. and al. ,2012)	C-F Present	**C-F (Dong, W. and al. ,2012)**
0.2	$\overline{\omega_1}$	21.019	21.02	14.485	-	9.272	10.05	3.303	3.30
	$\overline{\omega_2}$	57.941	57.94	46.942	-	37.090	37.09	20.702	20.70
	$\overline{\omega_3}$	113.589	113.59	97.942	-	83.453	84.28	57.965	57.97
1	$\overline{\omega_1}$	22.373	22.37	15.418	-	9.869	9.87	3.516	3.52
	$\overline{\omega_2}$	61.673	61.67	49.964	-	39.478	39.48	22.034	22.03
	$\overline{\omega_3}$	120.903	120.90	104.24	-	88.826	88.83	61.697	61.70
5	$\overline{\omega_1}$	21.019	21.02	14.485	-	9.272	10.05	3.0303	3.30
	$\overline{\omega_2}$	57.941	57.94	46.942	-	37.090	37.09	20.702	20.70
	$\overline{\omega_3}$	113.589	113.59	97.942	-	83.453	84.28	57.965	57.97

The no dimensional frequencies are compared to those reported in the literature. We remark that our results are in great agreement with the results previously published in the reference (Dong, W. and al., 2012), therefore validating the correctness of our constructed model. We can see that the eigenfrequencies of a clamped-clamed E-FGM beam (C-C) are more essential than the eigenfrequencies for the other bearing circumstances. The eigenfrequencies of a clamped-free E-FGM beam (C-F) are lower than those of the other bearing situations (C-F, C-S, S-S), independent of stiffness ratio values E1/E2. In addition to the various bearing conditions, the most relevant eigenfrequencies are those of isotropic and homogeneous beams ($E_1/E_2=1$). It should also be noted that the eigenfrequencies for stiffness ratio values $E_1/E_2 = 0.2$ and E1/E2 = 5 are same, independent of bearing circumstances, because they have the same rigidity. Table 2 displays the first three fundamental frequencies of a beam in P-FGM and S-FGM under various boundary conditions, with volume fraction indices ranging from "p = 0.1, 0.2, 0.5, 1, 2, 5, 10".

Table 3. Comparison of the frequencies ($\overline{\omega_n}$) between the P-FGM and S-FGM beams.

p	$\overline{\omega_n}$	C-C		C-S		S-S		C-F	
		S-FGM	P-FGM	S-FGM	P-FGM	S-FGM	P-FGM	S-FGM	P-FGM
0.1	$\overline{\omega_1}$	36.754	26.368	25.328	18.171	16.213	11.632	5.776	4.144
	$\overline{\omega_2}$	101.31	72.684	82.080	58.886	64.853	46.527	36.197	25.969
	$\overline{\omega_3}$	198.61	142.49	171.25	122.86	145.92	104.69	101.35	72.713
0.2	$\overline{\omega_1}$	36.484	28.414	25.143	19.581	16.094	12.535	5.734	4.465
	$\overline{\omega_2}$	100.57	78.325	81.478	63.456	64.378	50.138	35.932	27.984
	$\overline{\omega_3}$	197.15	153.55	170.00	132.40	144.85	112.81	100.60	78.356
0.5	$\overline{\omega_1}$	35.414	31.484	24.405	21.697	15.622	13.889	5.565	4.948
	$\overline{\omega_2}$	97.620	86.788	79.088	70.312	62.489	55.555	34.878	31.008
	$\overline{\omega_3}$	191.38	170.14	165.01	146.70	140.60	125.00	97.659	86.822
1	$\overline{\omega_1}$	33.830	33.830	23.314	23.314	14.924	14.924	5.316	5.316
	$\overline{\omega_2}$	93.254	93.254	75.551	75.551	59.694	59.694	33.318	33.318
	$\overline{\omega_3}$	182.82	182.82	157.63	157.63	134.31	134.31	93.291	93.291
2	$\overline{\omega_1}$	31.992	36.119	22.047	24.891	14.113	15.933	5.028	5.676
	$\overline{\omega_2}$	88.188	99.562	71.446	80.661	56.451	63.732	31.508	35.572
	$\overline{\omega_3}$	172.88	195.18	149.07	168.29	127.02	143.40	88.223	99.601
5	$\overline{\omega_1}$	30.342	39.088	20.910	26.937	13.385	17.243	4.768	6.142
	$\overline{\omega_2}$	83.639	107.75	67.761	87.292	53.539	68.971	29.882	38.496
	$\overline{\omega_3}$	163.97	211.23	141.38	182.13	120.46	155.19	83.672	107.79
10	$\overline{\omega_1}$	29.836	41.073	20.561	28.305	13.162	18.119	4.689	6.455
	$\overline{\omega_2}$	82.245	113.22	66.631	91.725	52.647	72.744	29.384	40.451
	$\overline{\omega_3}$	161.23	221.95	139.02	191.38	118.46	163.07	82.278	113.26

According to Table 3, it can be seen that the increase in the eigenfrequencies of a beam in FGM is related to the increase in the number of modes, and this is valid for different boundary conditions. As well as the eigenfrequencies fundamental of the S-FGM beams increase with the decrease in the volume fraction index "p"; on the other hand, the eigenfrequencies Fundamental of the P-FGM beams increase with the increase in the volume fraction index "p".
The figures 5, 6, 7, 8, 9, 10, 11 and 12 show the influence of the variation of "p" on the eigenfrequencies of an FGM beam in a mixture of AL/AL_2O_3 through the thickness "h" of the beam.

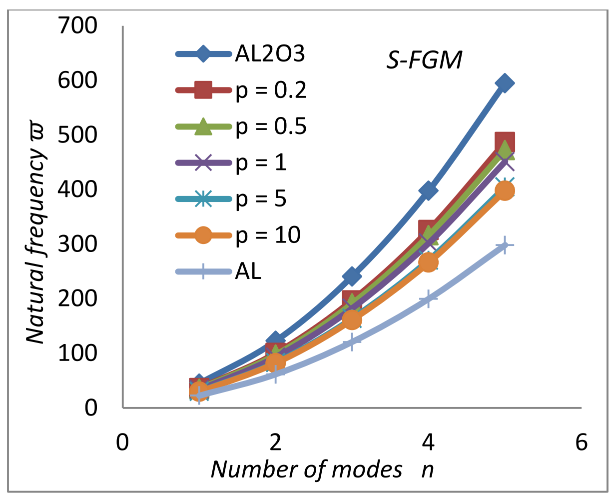

Figure 5. Eigenfrequencies of a clamped–clamped beam

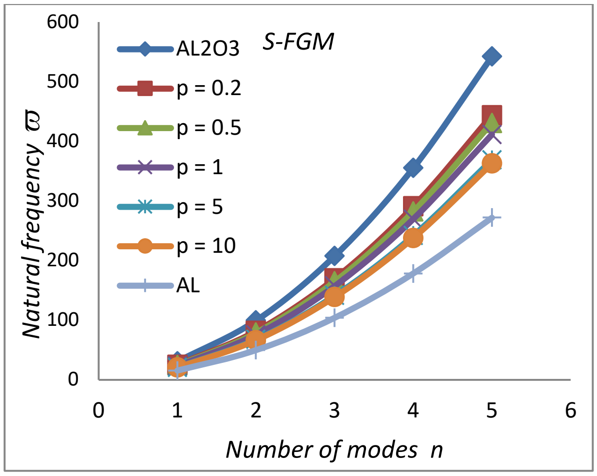

Figure 6. Eigenfrequencies of a clamped– supported beam

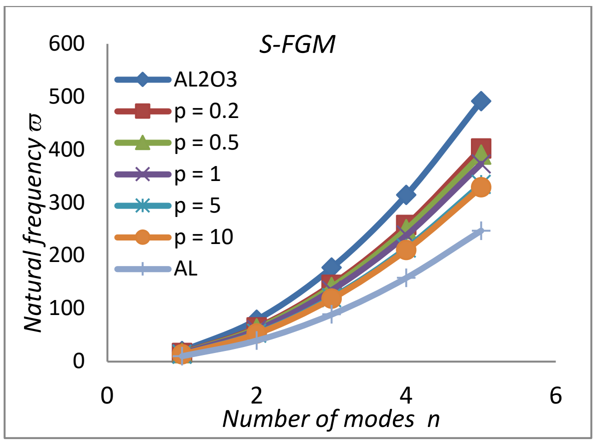

Figure7. Eigenfrequencies of a supported – supported beam.

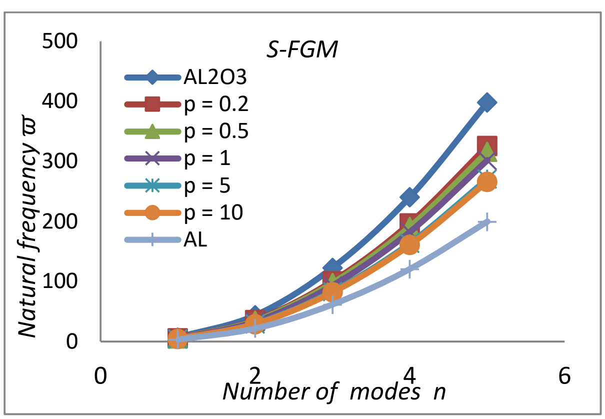

Figure 8. Eigenfrequencies of a clamped–free beam

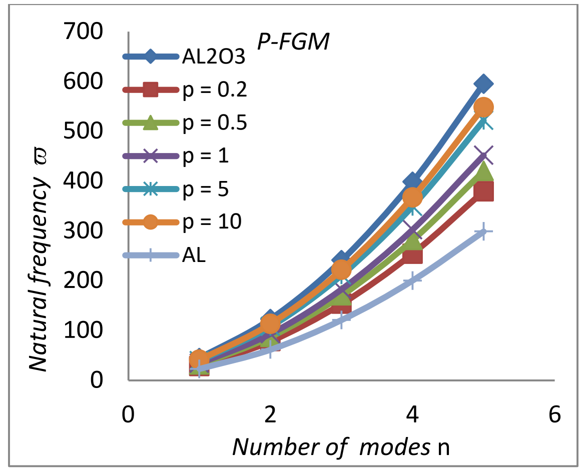

Figure 9. Eigenfrequencies of a clamped–clamped beam

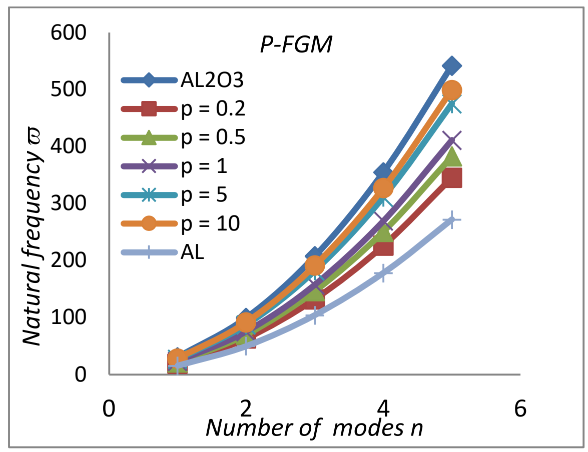

Figure 10. Eigenfrequencies of a clamped– supported beam.

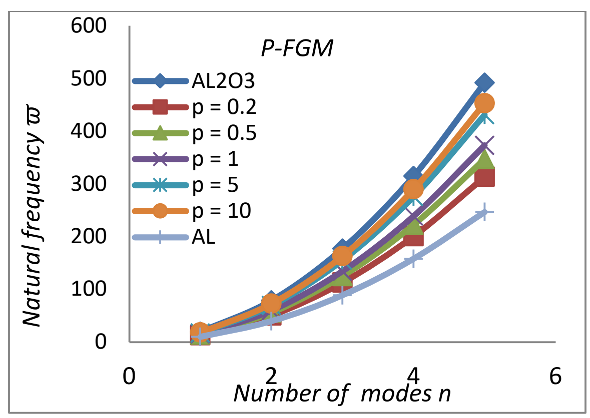

Figure 11. Eigenfrequencies of a supported – supported beam.

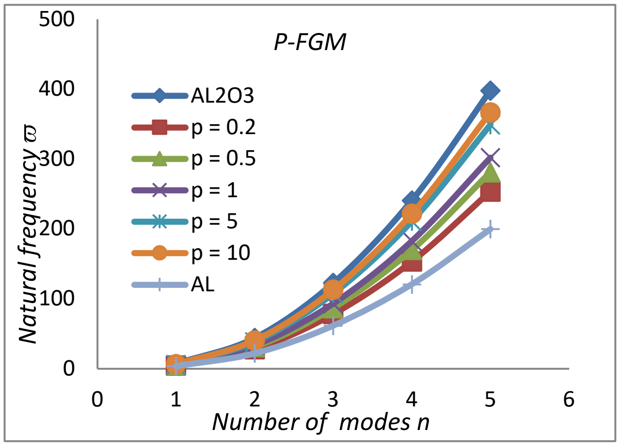

Figure 12. Eigenfrequencies of a clamped–free beam.

The figures 5, 6, 7, 8, 9, 10, 11 and 12 represent the evolution of the eigenfrequencies as a function of the number of vibration modes of a beam in FGM, for different boundary conditions. The volume fraction index "p" is varied by 0,1, 0,2, 0,5, 1, 2, 5 to 10 to see the influence of these volume fractions on eigenfrequencies. Based on the analysis of these figures, it can be seen that for the four bearing conditions, the increase in the eigenfrequencies of a beam in FGM is linked to the increase in the number of modes. Therefore, it can be deduced that the increase in the number of modes has a significant effect on the increase in eigenfrequencies in FGM. We also observed that the eigenfrequencies are maximum for ceramic beams (100%) and minimum for metal beams (100%). It can be seen that the eigenfrequencies increase when the rigidity of the material increases, which is due to the increase in the amount of ceramics in the FGM beams. The eigenfrequencies fundamental frequencies of the S-FGM beams increase with the decrease in the volume fraction index "p"; on the other hand, the eigenfrequencies fundamental of the P-FGM beams increase with the increase in the volume fraction index "p". It can be noted that the influence of the exponent "p" of the volume fraction is significant for (p> 1) and less significant for (p ≤ 1).

IV. COMPARISON BETWEEN S-FGM BEAMS, P-FGM AND E-FGM

The variation of the material properties of the FGM beam obeys the power law, exponential or a sigmoid distribution (P-FGM, E-FGM and S-FGM). The eigenfrequencies of the FGM beams will be compared with each other and also compared with the eigenfrequencies of an isotropic and homogeneous beam for different boundary conditions.

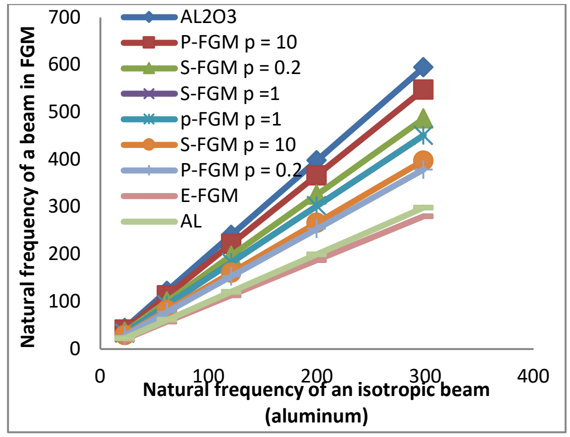

Figure 13. Eigenfrequencies of a clamped-clamped FGM beam compared to the eigenfrequencies of an isotropic beam

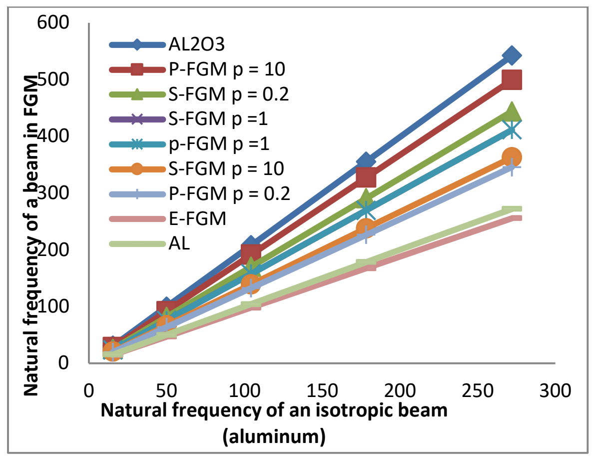

Figure 14. Eigenfrequencies of a clamped-supported FGM beam compared to the eigenfrequencies of a homogeneous beam

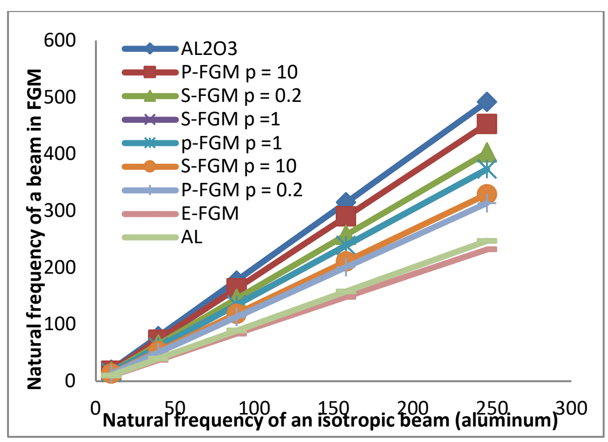

Figure 15. Eigenfrequencies of a supported - supported FGM beam compared to the eigenfrequencies of a homogeneous beam

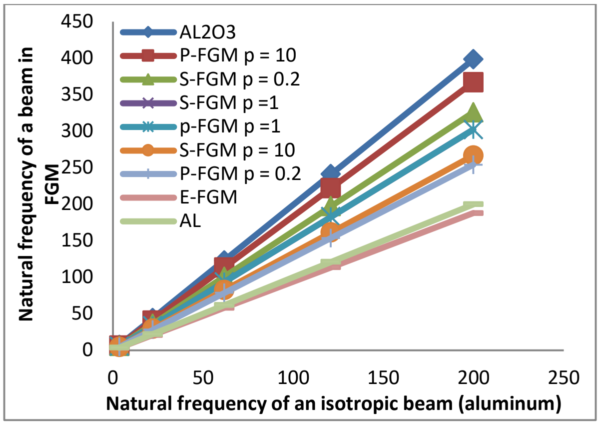

Figure 16. Eigenfrequencies of a clamped-free FGM beam compared to the eigenfrequencies of a homogeneous beam.

The figures 13, 14, 15 and 16 show the direct proportionality between the eigenfrequencies of an FGM beam and those of an isotropic beam. Based on these numbers, it can be concluded that the P-FGM beam's eigenfrequencies with a volume fraction index of "p = 10" are the most significant eigenfrequencies of the FGM beam. This is because of the Beam's high Young's modulus, which is independent of bearing circumstances. Additionally, the E-FGM beam has less stiffness than a metal beam made of aluminium. Additionally, it is evident that the volume fraction "p" has a negligible impact on the S-FGM beam's eigenfrequencies in comparison to the P-FGM beam's Eigen frequencies. P-FGM and S-FGM beams have the same resistance modulus when "p = 1".

V. CONCLUSION

This study, we focused on deriving analytical solutions for the vibratory behavior of functionally graded beams (FGM) composed of Al/Al_2O_3, utilizing the Euler-Bernoulli beam theory. The material properties were assumed to vary along the beam's thickness according to power-law, exponential, and sigmoid distributions (P-FGM, E-FGM, and S-FGM). The equation of motion was formulated using the principle of virtual work, and the solutions were obtained by solving an eigenvalue problem. Initially, the model was validated by comparing our results with existing data from the literature for an E-FGM beam, confirming its accuracy. Subsequently, we examined the influence of material parameters on the eigenfrequencies of the FGM beams. The key findings of this study are as follow:

- The FGM beam's inherent frequencies are related to its stiffness.
- Natural frequencies vary based on the volume percentages of the ceramic-metal mixture.
- The eigenfrequencies of the S-FGM beam are less affected by the volume fraction "p" than those of the P-FGM beam.
- Compared to an S-FGM or P-FGM beam, the E-FGM beam has lower eigenfrequencies.
- The greatest eigenfrequencies are positively impacted by the volume fractions of the FGM material.

Although this work provides valuable insights into the vibration behavior of the FGM beams, it is limited to room-temperature environments. Structures often operate under varying thermal and environmental conditions, which can significantly alter their mechanical and vibration characteristics. Therefore, future studies should focus on the combined effects of thermal gradients. Such studies are essential for developing more accurate models and ensuring the reliable performance of the FGM structures under real-world operating conditions.

AUTHOR CONTRIBUTIONS

A. Elhannani: Conceptualization, Methodology, Validation, Writing – original draft, Writing – review & editing. **R. Brahami:** Software, Data curation, Visualization, Writing – review & editing. **A. Elmeiche:** Formal analysis, Validation, Writing – review & editing. **M. Bouamama:** Supervision, Project administration, Writing – review & editing. **A. Rabehi:** Writing – original draft, Literature review, Writing – review & editing. **M. Benghanem:** Supervision, Funding acquisition, Writing – review & editing.

ACKNOWLEDGEMENT(S)

The researchers wish to extend their sincere gratitude to the Deanship of Scientific Research at the Islamic University of Madinah (KSA) for the support provided to the Post-Publishing Program.

REFERENCES

Ghorbanpour Arani, A. A., Niknejad, S., & Abbasian Arani, A. A. (2021). Dynamic response of Bi-directional functionally graded materials (BDFGMs) beams rested on visco-pasternak foundation under periodic axial force. *Journal of Solid Mechanics*, *13*(3), 269-285.

Bagheri, H., Kiani, Y., & Eslami, M. R. (2023). Geometrically nonlinear response of FGM beams on elastic foundation subjected to thermal shock. *Iranian Journal of Science and Technology, Transactions of Mechanical Engineering*, *47*(1), 187-201.

Belarbi, M. O., Khechai, A., Houari, M. S. A., Bessaim, A., Hirane, H., & Garg, A. (2024). Free vibration behavior of sandwich FGM beams: parametric and uncertainty analysis. *Journal of Vibration Engineering & Technologies*, *12*(Suppl 1), 883-905.

Chi, S. H., & Chung, Y. L. (2006). Mechanical behavior of functionally graded material plates under transverse load—Part I: Analysis. *International Journal of Solids and Structures*, *43*(13), 3657-3674.

Chikh, A. (2019). Analysis of static behavior of a P-FGM Beam. *Journal of Materials and Engineering Structures «JMES»*, *6*(4), 513-524.

Das, P., Benslimane, A., Islam, M. A., Mondal, D., & Nazim, M. S. (2024). A thermo-mechanically loaded rotating FGM cylindrical pressure vessels under parabolic changing properties: An analytical and numerical analysis. *Heliyon*, *10*(4), e25969.

Delale, F., & Erdogan, F. (1983). The crack problem for a nonhomogeneous plane, *J. Appl. Mech.*50 (3), 609-614.

Wei, D., Liu, Y., & Xiang, Z. (2012). An analytical method for free vibration analysis of functionally graded beams with edge cracks. *Journal of Sound and Vibration*, *331*(7), 1686-1700.

Elhannani, A., Refassi, K., Elmeiche, A., & Bouamama, M. (2019). Vibration analysis of functionally graded tapered rotor shaft system. *Mechanics and Mechanical Engineering*, *23*(1), 241-245.

Elmeiche, A., Bouamama, M., Elhannani, A., Belaziz, A., & Hammoudi, A. (2022). Dynamic modeling of functionally graded beams undergoing mobile mass. *Materials Physics & Mechanics*, *48*(1), 91-105

Esen, I. (2019). Dynamic response of functional graded Timoshenko beams in a thermal environment subjected to an accelerating load. *European Journal of Mechanics-A/Solids*, *78*, 103841.

Gayen, D. (2024). Thermo-elastic buckling and free vibration behavior of functionally graded beams with various materials gradation laws. *International Journal on Interactive Design and Manufacturing (IJIDeM)*, 1-20. https://doi.org/10.1007/s12008-024-02141-1.

Ghorbanpour Arani, A., & Niknejad, S. (2020). Dynamic stability analysis of Euler-Bernoulli and Timoshenko beams composed of bi-directional functionally graded materials. *AUT Journal of Mechanical Engineering*, *4*(2), 201-214.

Hadji, L., Daouadji, T. H., & Bedia, E. A. (2016). Dynamic behavior of FGM beam using a new first shear deformation theory. *Earthquakes and Structures*, *10*(2), 451-461.

Jabbar, N. A., Hussain, I. Y., Abdullah, O. I., & Mohammed, M. N. (2024). Finite element analysis of the thermal and thermo-mechanical coupling problems in the dry friction clutches using functionally graded material. *Curved and Layered Structures*, *11*(1), 20240001.

Karabulut, Ş., Karakoc, H., Bilgin, M., Canpolat, H., Krolczyk, G. M., & Sarıkaya, M. (2023). A comparative study on mechanical and ballistic performance of functionally graded Al6061 composites reinforced with B4C, SiC, and Al2O3. *Journal of Materials Research and Technology*, *23*, 5050-5065.

Liu, Z., Nie, M., Yue, T., Jiang, P., Li, X., & Zhang, Z. (2024). Directed energy deposition of functional gradient material to enhance mechanical properties of heterogeneous stainless steels. *Optics & Laser Technology*, *179*, 111326.

Ma, Z., Liu, W., Li, W., Liu, H., Song, J., Liu, Y., ... & Zhang, Y. (2024). Additive manufacturing of functional gradient materials: A review of research progress and challenges. *Journal of Alloys and Compounds*, *971*, 172642.

Mechab. (2011). Study of composite structures using high order theories under thermomechanical loading. Doctoral Thesis, Djilali Liabes University, Sidi Bel Abbes.

Mesbah, A., Belabed, Z., Amara, K., Tounsi, A., Bousahla, A. A., & Bourada, F. (2023). Formulation and evaluation a finite element model for free vibration and buckling behaviours of functionally graded porous (FGP) beams.*Structural Engineering and Mechanics,86(3)*,291-309.

Mishra, A. K., Yadav, K., & Kumar, A. (2023). Selective laser melting of functionally graded material: Current trends and future prospects. In *Advances in Additive Manufacturing* (pp. 281-297). Elsevier.

Priyanka, R., Twinkle, C. M., & Pitchaimani, J. (2022). Stability and dynamic behavior of porous FGM beam: influence of graded porosity, graphene platelets, and axially varying loads. *Engineering with Computers*, *38*(Suppl 5), 4347-4366.

Quang, V. D., Khoa, N. D., & Duc, N. D. (2021). The effect of structural characteristics and external conditions on the dynamic behavior of shear deformable FGM porous plates in thermal environment. *Journal of Mechanical Science and Technology*, *35*(8), 3323-3329.

Su, X., Hu, T., Zhang, W., Kang, H., Cong, Y., & Yuan, Q. (2024). Transfer matrix method for free and forced vibrations of multi-level functionally graded material stepped beams with different boundary conditions. *Applied Mathematics and Mechanics*, *45*(6), 983-1000.

Tüfekci, M., Dear, J. P., & Salles, L. (2024). Forced vibration analysis of beams with frictional clamps. *Applied Mathematical Modelling*, *128*, 450-469.